Evidence for a role of human blood-borne factors in mediating age-associated changes in molecular circadian rhythms

Authors: Jessica E. Schwarz[1,2], Antonijo Mrčela[3], Nicholas F. Lahens[3], Yongjun Li[2], Cynthia T. Hsu[1,2], Gregory Grant[3,4], Carsten Skarke[2,3], Shirley L. Zhang[1,2,5*], and Amita Sehgal[1,2*]

Affiliations:

[1]Howard Hughes Medical Institute, Perelman School of Medicine, University of Pennsylvania; Philadelphia, PA 19104, United States.

[2]Chronobiology and Sleep Institute, Perelman School of Medicine, University of Pennsylvania; Philadelphia, PA 19104, United States.

[3]Institute for Translational Medicine and Therapeutics (ITMAT), Perelman School of Medicine, University of Pennsylvania; Philadelphia, PA 19104, United States.

[4]Department of Genetics, Perelman School of Medicine, University of Pennsylvania; Philadelphia, PA 19104, United States.

[5]Current Institution: Department of Cell Biology, Emory University School of Medicine; Atlanta, GA 30323, United States.

*Email: Amita Sehgal, amita@pennmedicine.upenn.edu ; Shirley L. Zhang, shirley.zhang2@emory.edu

Author Contributions: Conceptualization, J.E.S. and A.S.; Methodology, J.E.S, A.M., N.F.L., Y.L., C.T.H., G.G., C.S., S.L.Z, and A.S.; Formal Analysis, J.E.S, S.L.Z, A.M., N.F.L., Y.L., and C.T.H; Investigation, J.E.S, S.L.Z., and C.S.; Writing – Original Draft Preparation, J.E.S. and A.S.; Writing – Review & Editing, J.E.S, A.M., N.F.L., Y.L., C.T.H., G.G., C.S., S.L.Z, and A.S.; Visualization, J.E.S., A.M, N.F.L.; Supervision, S.L.Z and A.S.

ABSTRACT

Aging is associated with a number of physiologic changes including perturbed circadian rhythms; however, mechanisms by which rhythms are altered remain unknown. To test the idea that circulating factors mediate age-dependent changes in peripheral rhythms, we compared the ability of human serum from young and old individuals to synchronize circadian rhythms in culture. We collected blood from apparently healthy young (age 25-30) and old (age 70-76) individuals and used the serum to synchronize cultured fibroblasts. We found that young and old sera are equally competent at driving robust ~24h oscillations of a luciferase reporter driven by clock gene promoter. However, cyclic gene expression is affected, such that young and old sera drive cycling of different genes. While genes involved in the cell cycle and transcription/translation remain rhythmic in both conditions, genes identified by STRING and IPA analyses as associated with oxidative phosphorylation and Alzheimer's Disease lose rhythmicity in the aged condition. Also, the expression of cycling genes associated with cholesterol biosynthesis increases in the cells entrained with old serum. We did not observe a global difference in the distribution of phase between groups, but find that peak expression of several clock controlled genes (*PER3, NR1D1, NR1D2, CRY1, CRY2,* and *TEF*) lags in the cells synchronized with old serum. Taken together, these findings demonstrate that age-dependent blood-borne factors affect peripheral circadian rhythms in cells and have the potential to impact health and disease via maintaining or disrupting rhythms respectively.

INTRODUCTION

Circadian rhythms are known to regulate homeostatic physiology including sleep:wake, hormone production and body temperature, and their dysregulation with aging is accompanied by adverse health consequences[1–3], raising the possibility that health decline with age is caused in part by circadian dysfunction. Although the mechanisms responsible for age effects on

53 circadian rhythms are unknown, signals from the central clock in the suprachiasmatic nucleus
54 (SCN) dampen with age[3–5] and rhythms change in peripheral tissues in different ways[5,6]. Here
55 we aimed to develop a culture model to study the effect of aging on human rhythms of
56 peripheral tissues. Given that serum can reset the clock in peripheral fibroblasts[7], we
57 questioned the extent to which serum factors normally contribute to peripheral rhythms of gene
58 expression and how they might affect rhythms with age, given that blood-borne factors can
59 influence other aspects of aging[8].

60 We collected blood samples from young (age 25-30) and old (age 70-76) apparently
61 healthy individuals following observations of their behavior and physiology, and tested the
62 hypothesis that age-dependent factors in the sera affect the core clock or outputs of the core
63 clock in cultured fibroblasts. In support of this theory, here we show that genes associated with
64 oxidative phosphorylation and mitochondrial functions lose rhythmicity in the presence of aged
65 serum factors. We also find that the expression of several molecular clock genes (*PER3,*
66 *NR1D1, NR1D2, CRY1, CRY2* and *TEF*) is phase delayed when synchronized with aged serum.
67 These novel findings suggest that it may be possible to treat impaired circadian physiology and
68 the associated disease risks by targeting blood borne factors.

69

70 **RESULTS**

71 We enrolled 8 old and 7 young human subjects (Fig.1A), whose demographics are in
72 Table S1. Midline Estimating Statistic of Rhythm: a rhythm-adjusted mean (MESOR) data
73 obtained from wearable EKG demonstrated that heart rate in old subjects trended lower with
74 increased variability (Fig. 1B&C). Young subjects displayed a trend of higher activity in the
75 sympathetic nervous system (SNS), and lower activity in the parasympathetic nervous system
76 (PNS) (Fig S1A), with no significant difference in cortisol levels (Fig S1B).

To monitor rhythms in culture, *BMAL1-luciferase* transfected BJ-5TA fibroblasts[9] were synchronized with old/young serum[7,10,11], and circadian effects were assessed by luciferase assay[9] over 4 days (Fig S2A). No significant differences were observed in the period, amplitude, and phase of the *BMAL1-luciferase* rhythm with young versus old serum treatment (Fig S2B).

To assess serum effects on circadian gene expression, we first performed RNA-seq around-the-clock on fibroblasts synchronized with serum from a single old or single young individual and found that, compared to the first day of synchronization (CT12-34), the second day (CT 36-58) showed greater differences in MESORs between young and old serum-treated groups (Fig. S3). This is not surprising because the first day includes acute responses of the fibroblasts to serum, which can mask circadian rhythms, and so the second day is expected to reveal differences in endogenous rhythms between samples. Day 2 also revealed different phases of cyclic expression between young and old groups for a larger number of genes. We proceeded to collect fibroblasts synchronized by sera from eight different subjects (four old, four young with two male and two female per group) at two-hour intervals, from 32 to 58 hours post serum addition. This added an extra two timepoints to the second day to facilitate the calculation of rhythmicity. Using CircaCompare[12] and a weighted BIC>0.75 cutoff, a significant number of genes were found to lose (1519 genes) or gain (637 genes) rhythmicity with age, underscoring the impact of age on the ability of serum to synchronize circadian rhythms, while 1209 genes were rhythmic in both groups (Fig 2A). Additionally, we used CircaCompare to estimate MESORs, amplitudes, and phases of gene oscillatory patterns in young and old groups, and to compare these cosinor parameters between groups (Fig 2B). Of the genes that were rhythmic in both groups, many also showed changes with age. For instance, 568 cyclically expressed genes showed a change in MESOR with age ($q < 0.05$ for MESOR differences), with MESOR values increasing for 163 genes and decreasing for 405 genes in the old serum-treated samples. Using p-values provided by CircaCompare we were able to detect changes in

102 amplitude (Fig 2C) for only a small number of genes (39 genes had decreased amplitude in old
103 and 2 had increased amplitude). Using CircaCompare and a $q < 0.05$ cutoff for phase
104 differences in genes rhythmic in young and old, we detected 20 genes with advanced phase,
105 and 34 with delayed phase (Fig 2D).

106 Search Tool for the Retrieval of Interacting Genes (STRING)[13] and Ingenuity Pathway
107 Analysis (IPA)[14] were used for functional genomics, and both approaches indicate a
108 maintenance of cycling of cell cycle genes, and a loss of rhythmicity of genes associated with
109 oxidative phosphorylation in the aged serum (Fig 3 and S4). STRING analysis revealed that the
110 dominant pathways that are rhythmic in both young and old conditions, cell cycle and DNA
111 replication demonstrate a decrease in MESOR with old serum. Checkpoint control and
112 chromosomal replication pathways were expressed cyclically in both young and old conditions;
113 however, several chromosomal replication pathway genes exhibit decreased MESORs in the
114 aged sera (Fig S4 D,E, Table S2). MESORs of steroid biosynthesis genes, particularly those,
115 relating to cholesterol biosynthesis, were also increased in the old sera condition (Fig 3, Table
116 S3).

117 As noted, the pathways that lost rhythmicity in the old sera included oxidative
118 phosphorylation, implicating mitochondrial dysfunction. By STRING analysis, 24 out of the 26
119 genes associated with oxidative phosphorylation are also among the Alzheimer's Disease
120 STRING network highlighting the disease relevance of this class of genes that loses cycling in
121 older individuals. Given that Alzheimer's pathology is closely associated with the accumulation
122 of oxidative stress[15], it is possible that loss of cycling contributes to oxidative damage. An
123 additional 31 genes in the Alzheimer's Disease STRING network lose rhythmicity with aged
124 serum; these include amyloid precursor protein (APP) and apolipoprotein E (APOE). APP is by
125 definition the precursor of amyloid beta, which accumulates in AD[16]. While APOE plays an

important role in lipid transport, specific variants of this gene are strongly associated with AD risk as APOE interacts with amyloid beta in amyloid plaques, a hallmark of the disease [17].

Lastly, several clock genes showed differences in expression with the aged serum, most notably genes in the Circadian Rhythm KEGG pathway (Fig 4). In particular, expression of *CRY1*, *CRY2*, *NR1D1*, *NR1D2*, *PER3*, and *TEF* was significantly phase delayed after synchronization with old serum (Fig 4). Importantly, the RNA-seq did not reveal a difference in the phase or amplitude of *BMAL1* expression with age, supporting our *BMAL1-luciferase* findings, although the MESOR significantly increased with age.

DISCUSSION

Although studies of the aged SCN have revealed persistent cycling of clock gene expression but a breakdown of output signals[4,5], whether age-related changes in systemic signaling impact organismal clocks has yet to be elucidated. We demonstrate here that while the core clock continues to cycle in cultured fibroblasts synchronized with serum from old volunteers, the circadian transcriptome is different from that seen in cells treated with serum from young individuals. Through this analysis of the role of serum in age-induced changes in circadian rhythms, we suggest a potential mechanism for other studies, which showed that specific genes lose, gain, or maintain rhythmicity with age[18–22]. This phenomenon, known as circadian reprogramming, may illuminate which pathways are affected by or become more impactful for cellular maintenance through aging in a tissue specific manner[23]. Interestingly, many of the genes in the circadian transcriptome that exhibit age-related changes are independently implicated in aging. For instance, some of the genes that lose rhythmicity in the aged condition are involved in oxidative phosphorylation and mitochondrial function, both of which decrease with age[24,25]. We suggest that the age-related inefficiency of oxidative phosphorylation derives at least in part from loss of cycling due to changes in serum signals.

151 In order to study the effect of circulating factors on age-related changes of the circadian
152 transcriptome, we utilized the well-established serum starvation-serum addition protocol[7] to
153 synchronize cells in culture. Fibroblasts from old and young subjects have robust clocks and
154 respond similarly to synchronization with dexamethasone[10]; however, when synchronized with
155 dexamethasone in a media containing old serum, they exhibited shortened circadian periods[10].
156 This effect was reversed by heat inactivating old serum. We did not observe a significant
157 difference in period length between young and old serum synchronization in our *BMAL1-*
158 *luciferase* experiment, perhaps because of the absence of dexamethasone. Our use of serum to
159 synchronize allowed us to more closely simulate *in vivo* conditions where blood is an important
160 mode by which central clocks can entrain peripheral clocks to maintain synchrony with the
161 day:night cycle. Previously, serum factors were shown to activate the immediate early
162 transcription factor, SRF, in a diurnal manner to confer time of day signals to both cells in
163 culture and to mouse liver[7]. We show here that effects of age are also mediated by serum. We
164 find that while the number of rhythmic transcripts in the young serum condition (~10%) is higher
165 than the old serum condition (~4%), both conditions demonstrate a much larger number of
166 cycling transcripts in these cultured fibroblasts than in other cell culture studies[26–29]. However, in
167 mammals, up to 20% of transcripts can cycle in a given tissue[30,31], and the low number of
168 cycling transcripts in culture has been cited as a major limitation of the culture model[28]. A major
169 contributing factor to robust in vivo cycling might be human serum as the synchronization signal.
170 In this way, our model of mimicking signaling to peripheral tissues by using serum directly from
171 humans may more accurately recapitulate the human condition.

172 Together, these findings indicate that at least some of the age-related changes in the
173 circadian clock and circadian transcriptome are derived from signals circulating in the serum
174 and not the age of the tissue. This has profound implications for understanding and treating
175 circadian disruption with age, and could also be relevant for other age-related pathology, given

176 established links between circadian disruption and diseases of aging. Notably, many of the

177 genes whose cycling is affected by old serum contribute to age-associated disorders.

178 **FIGURES**

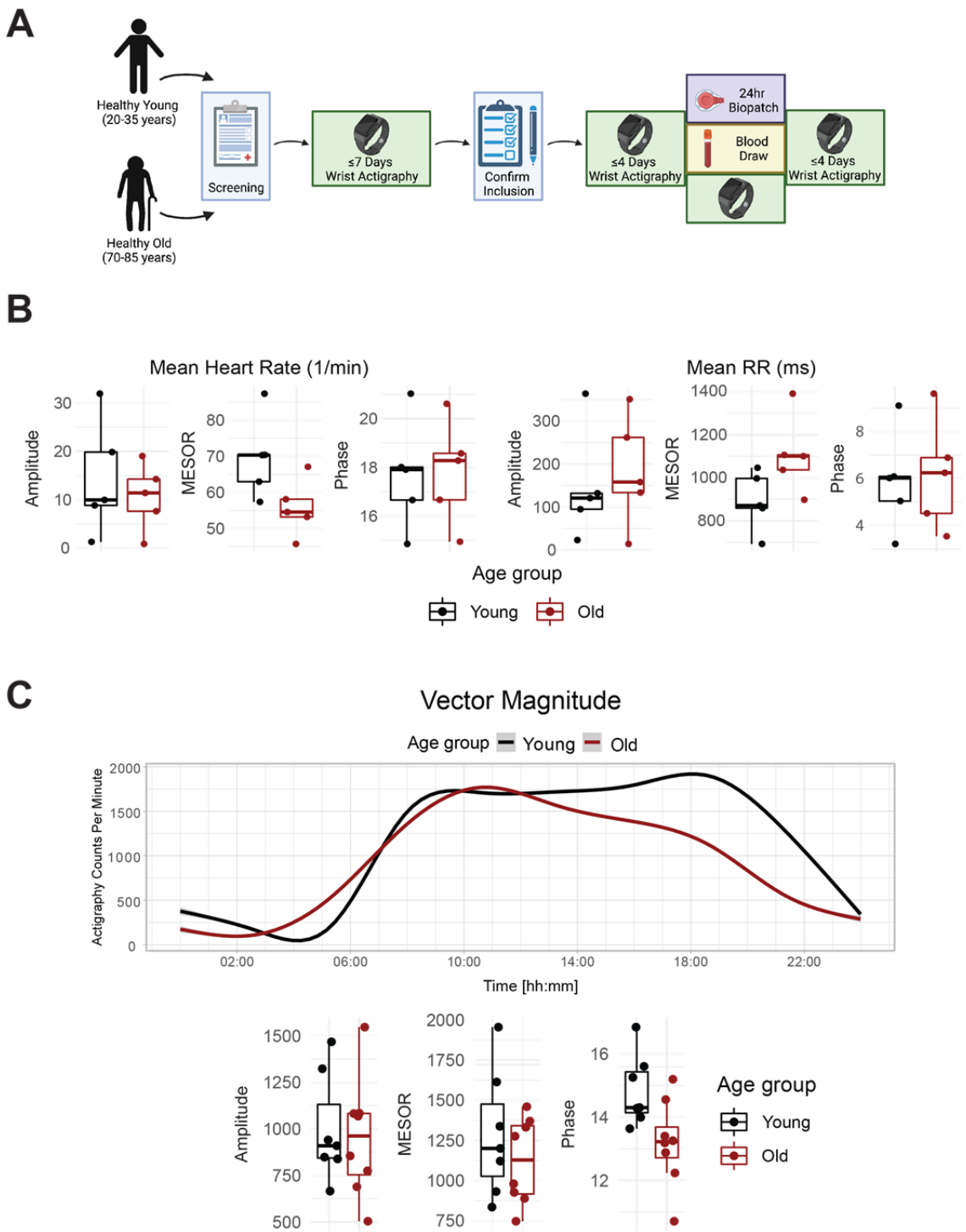

179

Fig 1. Healthy elderly individuals tend to have lower heart rate, increased heart rate variability, and phase advanced activity patterns relative to young subjects.

Experimental protocol for enrolment and monitoring of human subjects **(A)**. As assessed by Zyphyr BioPatch, EKG measurements suggest that MESOR of average heart rate decreases with age (p=0.056) and that MESOR of heart rate variability increases with age (p=0.056). N=5 per group. MESOR and amplitude were tested using two-sided Wilcoxon rank sum exact test, while phase was tested by Kuiper's two-sample test **(B)**. Average activity counts across three axes (vector magnitude), as recorded by the actigraph device plotted throughout the day (top) and analyzed for circadian rhythm (bottom) **(C)**. While the amplitudes of activity did not differ between the age groups, the older individuals trended towards an early phase (p~0.055, Kupier's two-sample test) compared to young individuals. N=7 for young and N=8 for old. Lines in the top panel of C are smoothed means (fit with penalized cubic regression splines) for data from each age group. Dots in the bottom panel of C are subject-level cosinor parameter estimates derived from cosinor fits to the actigaraphy data. Summary Figure (A) was made with BioRender.com. Boxplot midlines correspond to median values, while the lower and upper hinges correspond to the first and their quartiles, respectively. Boxplot whiskers extend to the smallest/largest points within 1.5 * IQR (Inter Quartile Range) of the lower/upper hinge.

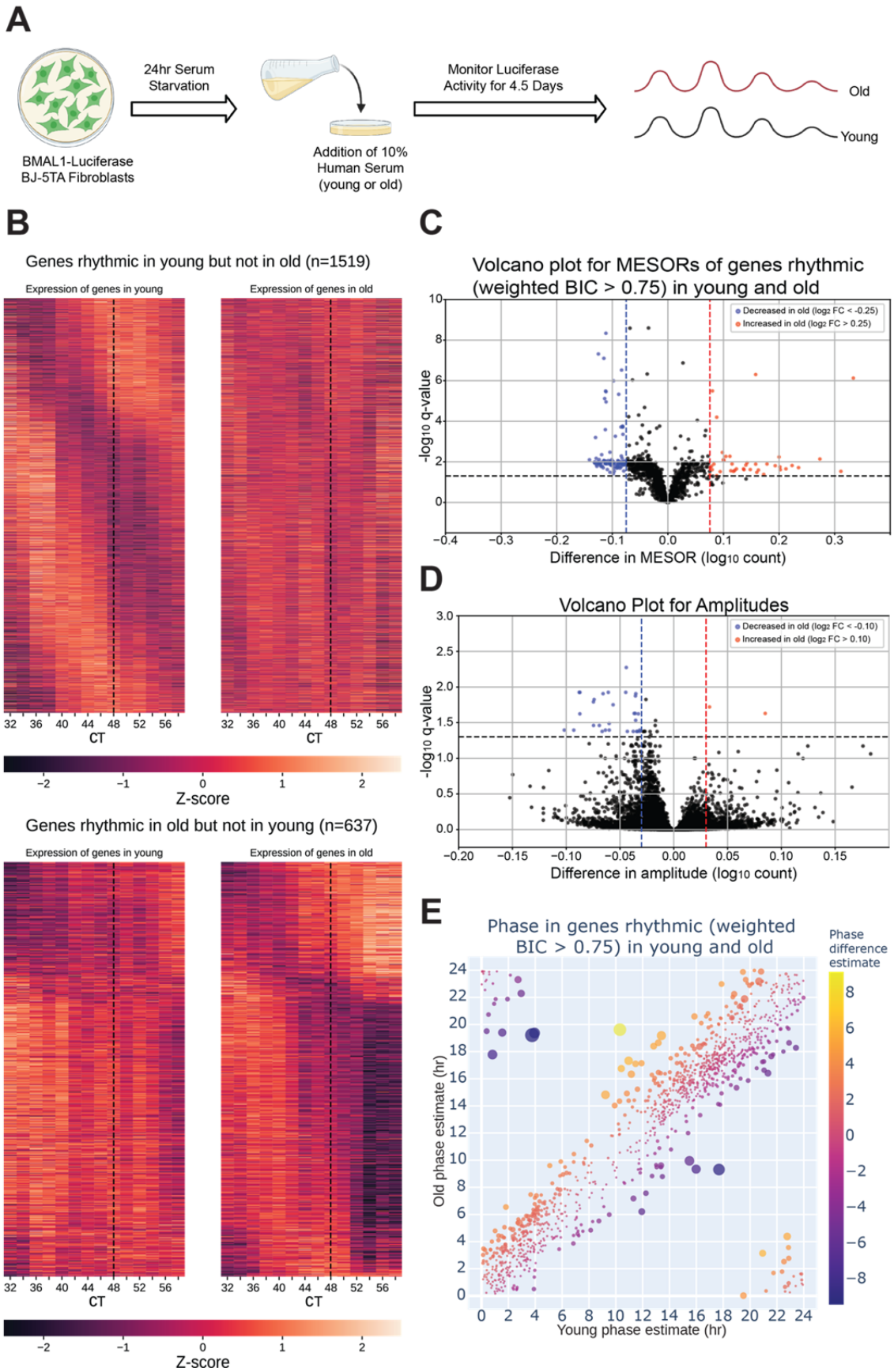
A
24hr Serum Starvation
Monitor Luciferase Activity for 4.5 Days
Old
Young
BMAL1-Luciferase BJ-5TA Fibroblasts
Addition of 10% Human Serum (young or old)
B
Genes rhythmic in young but not in old (n=1519)
Expression of genes in young
Expression of genes in old
CT
Z-score
Genes rhythmic in old but not in young (n=637)
C
Volcano plot for MESORs of genes rhythmic (weighted BIC > 0.75) in young and old
Decreased in old (log2 FC < -0.25)
Increased in old (log2 FC > 0.25)
-log10 q-value
Difference in MESOR (log10 count)
D
Volcano Plot for Amplitudes
Decreased in old (log2 FC < -0.10)
Increased in old (log2 FC > 0.10)
Difference in amplitude (log10 count)
E
Phase in genes rhythmic (weighted BIC > 0.75) in young and old
Phase difference estimate
Old phase estimate (hr)
Young phase estimate (hr)

198

199 **Fig 2. The circadian transcriptome is differentially affected by entrainment with sera from**
200 **young and old human subjects.**
201 A visual representation of the serum starvation-serum addition protocol to synchronize the
202 *BMAL1-luciferase* BJ-5TA fibroblasts **(A**, made with BioRender.com**)**. When comparing the
203 circadian transcriptome entrained by either young or old sera (n=4 sera per group), 1519 genes
204 lost rhythmicity with age (B, top) while only 637 genes gained rhythmicity with age (B, bottom).
205 Weighted BIC criterion with a threshold of 0.75 was used to assess rhythmicity **(B)**. The number
206 of genes rhythmic in young and old (according to weighted BIC > 0.75 criterion) that show a
207 detectable change in MESOR ($q < 0.05$ criterion for MESOR difference) is 568, with MESOR
208 increasing in 163 and decreasing in 405 genes. Out of these, 40 genes with increased MESOR
209 (red) and 98 genes with decreased MESOR (blue) also satisfy the condition $|\log_2 FC| > 0.25$
210 **(C)**. We were only able to detect change in amplitude for a small number of genes, 39 genes
211 had decreased amplitude in old and 2 had increased amplitude using CircaCompare. Only 30
212 genes with decreased amplitude also satisfy the condition $|\log_2 FC| > 0.1$ (blue) **(D)**. For phase,
213 using a test provided by CircaCompare, under $q < 0.05$ cutoff for age-related phase differences
214 in genes rhythmic in young and old (with BIC>0.75 cycling criteria), we detected 20 genes with
215 advanced phase, and 34 with delayed phase **(E)**.
216

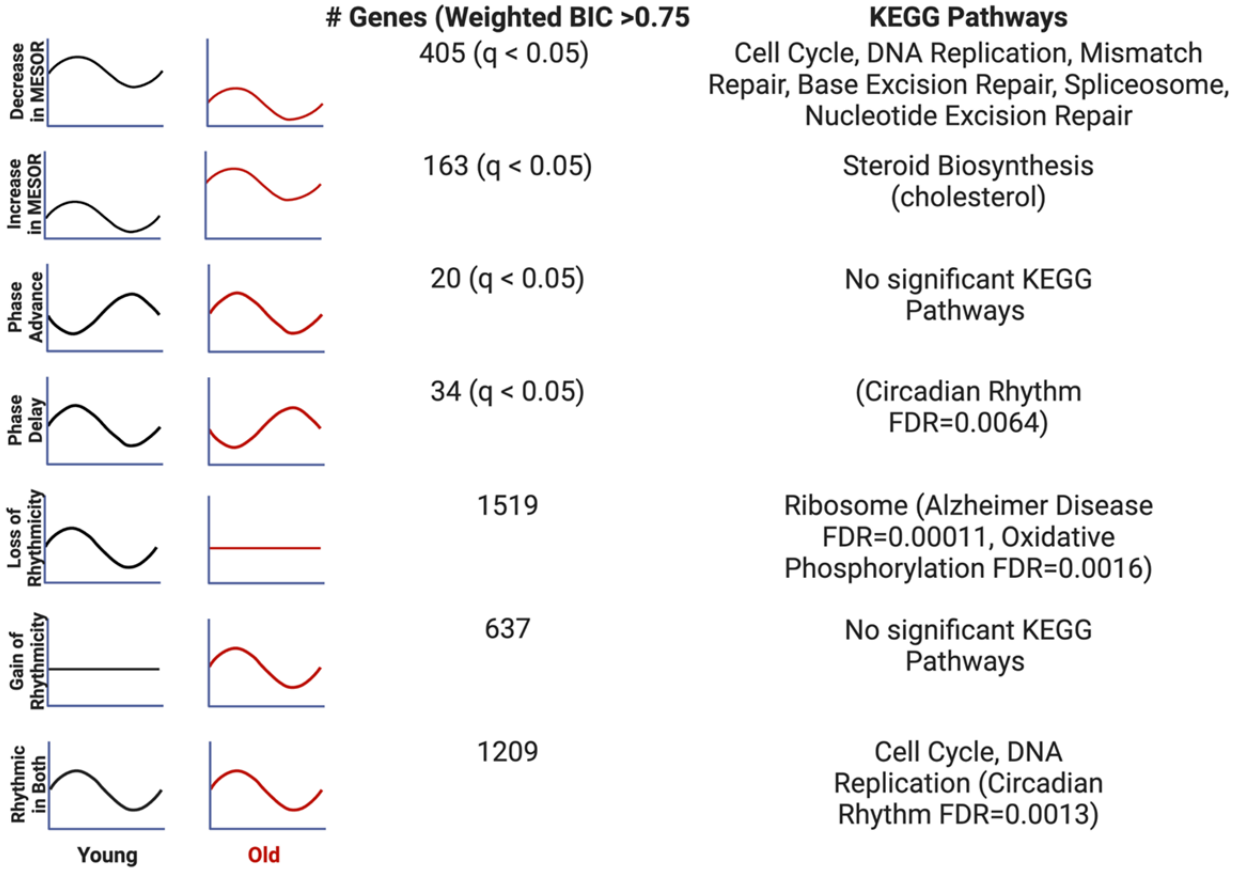

Fig 3. Each type of circadian change is associated with different KEGG pathways by STRING analysis

Entrainment of the fibroblasts in culture with old serum significantly altered the circadian transcriptome despite use of the same cells in both young and old conditions, suggesting the aged serum itself affects the regulation of specific pathways in the cell. Significant KEGG Pathways (FDR $<1\times10^{-4}$ unless specified) are indicated next to each category of genes. Age related pathways such as Alzheimer's Disease/oxidative phosphorylation are associated with a loss of rhythms in the old condition. Cell cycle and DNA replication pathways remain rhythmic in the old serum condition, but cycle with a decreased MESOR. Rhythmic genes were determined using CircaCompare. Rhythmicity was determined using the weighted BIC > 0.75 criterion while p-values for difference in MESOR and phase were determined using CircaCompare.

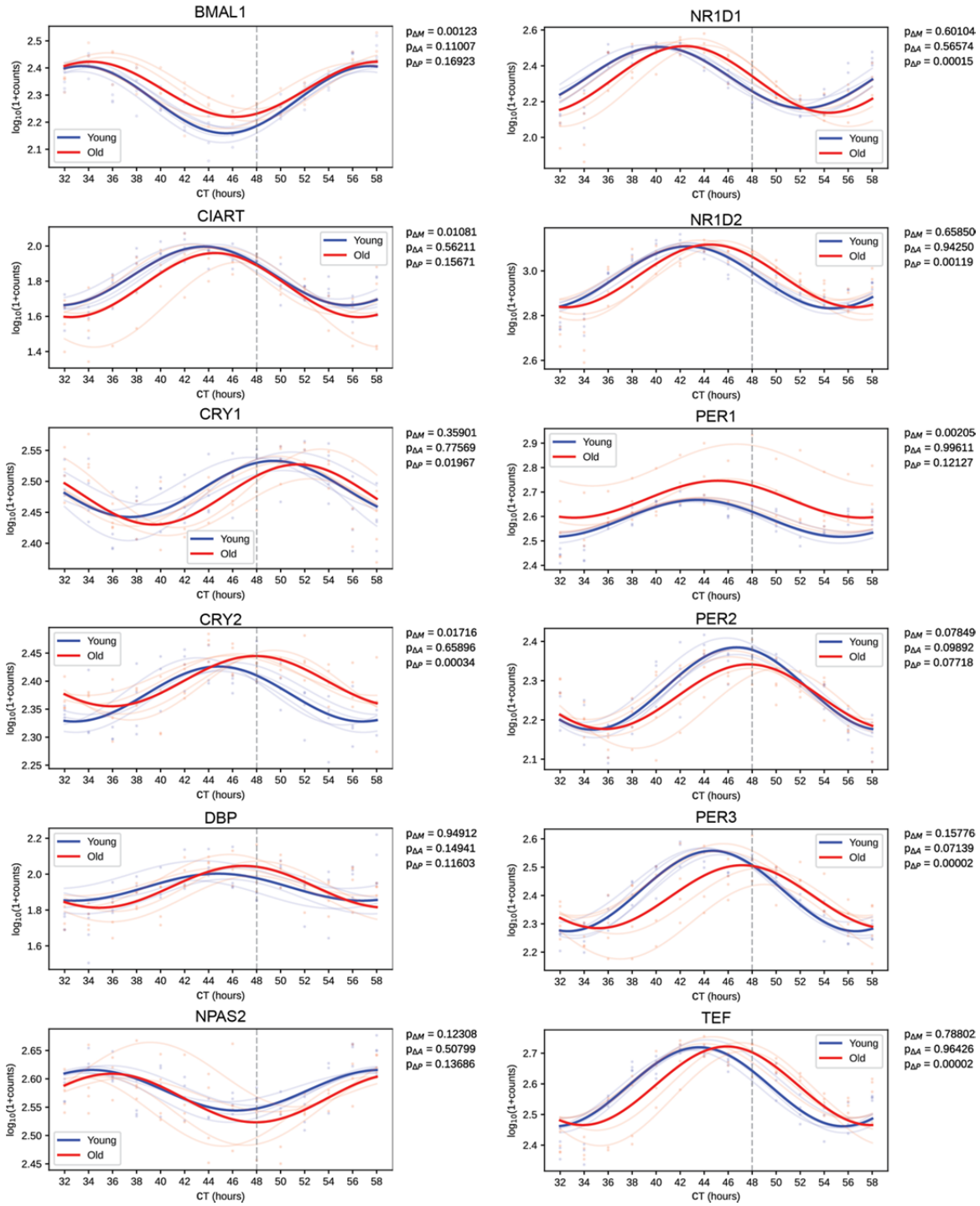

Fig 4. Synchronizing with old serum phase delays the expression profile of several core clock genes

Traces of molecular clock mRNA transcripts, the average curve (bold) of results of individual sera (faded). P-values for the difference in MESOR (P_**Δ**M), amplitude (P_**Δ**A), and phase

235 (P_**Δ**P) are shown for the comparison of young and old conditions. Several clock genes are
236 significantly phase delayed (*CRY1, CRY2, NR1D1, NR1D2, PER3, TEF*) in response to
237 synchronization with old serum. While *BMAL1* is not phase delayed, the MESOR significantly
238 increases with age. N=4 subjects per timepoint for both young and old groups.
239
240

MATERIALS AND METHODS

Clinical research study:

This clinical research study enrolled apparent healthy participants from the volunteer pool maintained by the Institute for Translational Medicine and Therapeutics (ITMAT), University of Pennsylvania. The Institutional Review Board of the University of Pennsylvania (Federal wide Assurance FWA00004028; IRB Registration: IORG0000029) approved the clinical study protocol (Penn IRB#832866). The study was registered on ClinicalTrials.gov with identifier NCT04086589. After obtaining informed consent from all volunteers, study assessments were conducted in the Center for Human Phenomic Science (Penn CHPS#3002) in accordance with relevant GCP guidelines and regulations. We originally intended on recruiting n=20 per group; however, patient recruitment was halted due to the COVID-19 pandemic. Participants met criteria for inclusion (in general good health, either 70-85 years of age for the elderly cohort or 20-35 years of age for the young cohort, and a wrist-actigraphy-based average TST (total sleep time) ≥ 6 hours per night occurring between 22:00 – 08:00). Participants were excluded due to pregnancy or nursing, shift work (defined as recurring work between 22:00-05:00), a history of clinically significant obstructive sleep apnea, transmeridian travel across ≥2 time zones in the two weeks prior to study assessments and one week after, > 2 drinks of alcohol per day, and use of illicit drugs. Blood collections were done from the median cubital vein via venipuncture using a 22 G butterfly needle (BD, Franklin, Lakes, NJ, USA). All blood draws occurred at 14:00, the same time as Pagani et al.[32]. One subject returned for a repeat clinical assessment including biosampling to provide additional sample.

Acquisition of accelerometry data streams:

Participants wore a triaxial actigraph device (wGT3X-BT, ActiGraph, Pensacola, FL) on the non-dominant wrist. The devices were initialized using the following parameters: start date and time were synchronized with atomic server time without pre-defined stop date/time, at 60

266 Hz sampling rate for the three accelerometer axes, enabled for delay modus, steps, lux,
267 inclinometer, and sleep while active. Raw data were downloaded from the device in AGD and
268 GT3X file format in one second epochs using ActiLife software (version 6, ActiGraph,
269 Pensacola, FL) and submitted for further analyses. For visualization and cosinor analysis,
270 actigraphy data were aggregated into 1-minute intervals by summing ActiGraph counts across
271 each minute. Cosinor analyses of the data were adapted from the single component cosinor
272 analysis reviewed by Cornelissen[33], as well as the cosine fit described by Refinetti et al. [34].
273 Briefly, the measurement times for the actigraphy data were recalculated as hours since
274 midnight on the first day of measurement, within each participant's data. For each actigraphy
275 variable and each participant, the lm() function in R (v4.2.0) was used to perform a cosinor fit
276 with a fixed 24-hour period. The two cosinor coefficients from these fits were used to calculate
277 participant-level amplitudes and circadian phases, while the intercepts provided MESOR
278 estimates. The two-sided Wilcoxon rank sum exact test, as implemented by R's wilcox.test()
279 function, was used to test for significant differences in amplitude and MESOR between the age
280 groups. A two-sample Kuiper's test, as implemented by the kuiper_test(nboots = 10000)
281 function from the twosamples R package (v2.0.0), was used to test for significant differences in
282 circadian phase between the age groups.

283 **Acquisition of EKG data:**

284 The Zephyr BioPatch devices (Zephyr Technology, Annapolis, MD) were deployed as
285 previously established[35]. All subjects included in this analysis wore the BioPatch for at least
286 24hrs. EKG recordings were analyzed by Kubios HRV Premium (ver. 3.5.0, Kubios Team,
287 Kuopio, Finland) to report time-of-day-specific measures of cardiovascular function consisting of
288 heart rate, RR intervals, sympathetic and parasympathetic nervous activity (SNS and PNS).
289 Preprocessing in Kubios was set to automatic beat correction to remove artifacts and Smoothn
290 priors for detrending. Cosinor fits and tests for differences in circadian parameters between age

291 groups were performed as described for the actigraphy data. The circadian parameters MESOR
292 and amplitude were tested for significant differences between the age groups by Wilcoxon rank
293 sum exact test (two-sided), while phase was tested by Kuiper's two-sample test to account for
294 the circular measurement.

295 **Cortisol Measurements:**

296 Cortisol was measured in human serum by coated tube RIA (MP Bio, Solon OH) in
297 duplicate. Tubes were counted on Perkin Elmer gamma counter and data reduced by STATLia
298 software.

299 **Generation of stable BJ-5TA cell line expressing *BMAL1-dLuc-GFP*[9]:**

300 Virus was generated and cells were infected as we've previously described[36]. Briefly,
301 LentiX 293T cells (Clonetech) were transfected with Lipofectamine 3000 PLUS (Life Tech) using
302 manufacturer instructions. The transfection included 18ug of DNA per reaction and the plasmid
303 (BMAL1-dLuc-GFP) to packaging vector (DVPR, Addgene) to envelope (VSV-G, Addgene) ratio
304 was 10:1:0.5. Media was changed 24hrs post-transfection after the cells were checked using a
305 fluorescence scope to make sure cells were >50% GFP positive. Supernatant with the virus was
306 collected at 48hrs and 72hrs post transfection and spun down at 3000 RPM for five minutes (to
307 eliminate any cells/debris). BJ-5TA cells were infected with fresh virus upon virus collection.
308 Polybrene (Sigma-Aldrich, 10 mg/mL) was also added to aid with infection. Transduced BJ-5TA
309 cells (>2000 cells) were sorted (FACSMelody, BD Biosciences) for high GFP expression. Once
310 the cell line was established, blasticidin was added to the culture at 2ug/ml. Due to fragility of
311 the cell line in the presence of antibiotic, BJ-5TA *Bmal1-luciferase* cells with differing expression
312 levels of GFP were sorted. The line with highest stable luminescence oscillation was used for all
313 experiments reported here.

314 **Serum entrainment and bioluminescent recording:**

315 BJ-5TA *BMAL1-dLuc-GFP* cells in 24-well plates (~confluent) were washed (2x) with
316 DPBS and given serum free media for 24hrs. After the starvation, cells were given media with
317 10% human serum and 200uM beetle luciferin potassium salt. Each well of cells was given
318 media with the serum from a single patient. The cells were continuously monitored by
319 LumiCycle luminometer (Actimetrics) for 4.5 days from the point of serum addition. LumiCycle
320 raw data was exported using LumiCycle software (Actimentrics). The data were analyzed by
321 BioDare2 (biodare2.ed.ac.uk[37]) using FFT NLLS with baseline detrending. Any replicates that
322 were not cycling or had a period outside of the 20-28hr range was excluded from analysis. Both
323 the serum free media and serum added media used the recipe from[9] at pH 7.4; however, the
324 serum free media had no serum and the serum media had 10% human serum instead of FBS.

325 **Sample preparation, RNA extraction, and RNA sequencing:**

326 BJ-5TA *BMAL1-dLuc-GFP* cells in 24-well plates (~confluent) were washed (2x) with
327 DPBS and given serum free media (DMEM with Penn Strep) for 24hrs. After 24hrs cells were
328 given media with human serum (DMEM, Penn Strep, 10% human serum). Serum starvation was
329 staggered every 12 hours over two days to allow for samples to be collected on the same day.
330 Upon sample collection wells were place on ice and rinsed with cold DPBS and then put in cold
331 RLT buffer with 2-Mercaptoethanol (10uL/mL). Samples were frozen at -80 overnight and sent
332 to Admera for RNA extraction and sequencing. Total RNA was extracted with RNeay mini kit
333 (Qiagen). Isolated RNA sample quality was assessed by High Sensitivity RNA Tapestation
334 (Agilent Technologies Inc., California, USA) and quantified by Qubit 2.0 RNA HS assay
335 (ThermoFisher, Massachusetts, USA). Paramagnetic beads coupled with oligo d(T)25 are
336 combined with total RNA to isolate poly(A)+ transcripts based on NEBNext® Poly(A) mRNA
337 Magnetic Isolation Module manual (New England BioLabs Inc., Massachusetts, USA). Prior to
338 first strand synthesis, samples are randomly primed (5´ d(N6) 3´ [N=A,C,G,T]) and fragmented
339 based on manufacturer's recommendations. The first strand is synthesized with the Protoscript

340 II Reverse Transcriptase with a longer extension period, approximately 40 minutes at 42°C. All
341 remaining steps for library construction were used according to the NEBNext® UltraTM II Non-
342 Directional RNA Library Prep Kit for Illumina® (New England BioLabs Inc., Massachusetts,
343 USA). Final libraries quantity was assessed by Qubit 2.0 (ThermoFisher, Massachusetts, USA)
344 and quality was assessed by TapeStation D1000 ScreenTape (Agilent Technologies Inc.,
345 California, USA). Final library size was about 430bp with an insert size of about 300bp.
346 Illumina® 8-nt dual-indices were used. Equimolar pooling of libraries was performed based on
347 QC values and sequenced on an Illumina® NovaSeq S4 Illumina, California, USA) with a read
348 length configuration of 150 PE for 40 M PE reads per sample (20 M in each direction).

349 **RNA-seq and statistical analysis**

350 Raw RNA-seq reads were aligned to the GRCh38 build of the human genome by STAR
351 version 2.7.10a[38]. The dataset contained an average of 19,265,220 paired-end non-stranded
352 150 bp reads mapping uniquely to genes, per sample. Data were normalized and quantified at
353 both gene and exon-intron level, using a downsampling strategy implemented in PORT
354 (Pipeline Of RNA-seq Transformations, available at https://github.com/itmat/Normalization),
355 version 0.8.5f-beta_hotfix1. Both STAR and PORT were provided with gene models from
356 release 106 of the Ensembl annotation[39].
357
358 MESOR, amplitude, and phase estimates, as well as p-values for the difference in
359 MESOR, amplitude, and phase, were calculated with CircaCompare[12], version 0.1.1. Only
360 rhythmic genes were taken into consideration in pathway and other analyses involving MESORs
361 and phases. The criterion for rhythmicity was either based on (BH adjusted) p-values reported
362 by CircaCompare, or weighted BIC values, obtained by an approach similar to dryR[40]. In the
363 latter approach we fitted four models of rhythmicity, one modeling gene expression that is
364 rhythmic in both cells treated with young or old sera, another modeling gene

365 expression rhythmic in neither cells treated with young nor old sera, and two modeling gene
366 expression rhythmic in either young or old sera treated cells respectively. The BIC values were
367 calculated for the four models and were weighted to obtain numbers between 0 and 1. All
368 methods were provided with $\log_{10}$(1 + PORT normalized count) values and were run on R,
369 version 4.1.2, accessed through Python, version 3.9.9, via rpy2, an interface to R running
370 embedded in a Python process, https://rpy2.github.io/, version 3.4.5. Additionally, we used
371 Nitecap[41] to visualize and explore circadian profiles of gene expression.
372
373 **STRING pathway analysis**
374 We performed STRING[13] pathway analyses using STRING API version 11.5.
375 Enrichment analyses were performed on the sets of genes rhythmic in both groups (weighted
376 BIC > 0.75) with observed decrease in MESOR, increase in MESOR, advance in phase, and
377 delay in phase according to CircaCompare q < 0.05 criterion. We also performed analyses on
378 the sets consisting of genes rhythmic only in young group (weighted BIC > 0.75), only in old
379 group (weighted BIC > 0.75), and the set of genes rhythmic in both groups (weighted BIC >
380 0.75). Finally, two additional analyses were performed, on the sets of genes with observed
381 decrease and increase of amplitude (CircaCompare q < 0.05).
382
383 **Ingenuity Pathway Analysis:**
384 QIAGEN IPA[14] was used to identify pathways enriched in various subsets of cycling
385 genes. The following subsets of genes were identified using a combination of CircaCompare
386 stats and BIC cutoffs: (1) Decreased MESOR in old sera (929 genes) – CircaCompare rhythmic
387 q < 0.05 in old, CircaCompare rhythmic q < 0.05 in young, CircaCompare MESOR difference q
388 < 0.05, MESOR difference (old – young) < 0. (2) Increased MESOR in old sera (515 genes) –
389 same selection criteria as 'Decreased MESOR in old sera,' except MESOR difference (old –

young) > 0. (3) Phase advance in old sera (148 genes) - CircaCompare rhythmic q < 0.05 in old, CircaCompare rhythmic q < 0.05 in young, CircaCompare Phase difference q < 0.05, phase difference (old – young) < 0. (4) Phase delay in old sera (156 genes) – same selection criteria as 'Phase advance in old sera,' except phase difference (old – young) > 0. (5) Loss of rhythmicity in old sera (1519 genes) – weighted BIC > 0.75 for 'Rhythmic in Young but not Old' model. (6) Gain of rhythmicity in old sera (637 genes) – weighted BIC > 0.75 for 'Rhythmic in Old but not Young' model. (7) Rhythmic in old and young sera (1209 genes) – weighted BIC > 0.75 for 'Rhythmic in both Old and Young' model. Each of these gene subsets were processed separately with IPA's core analysis, using default parameters.

For visualization via heatmap, we perform three rounds of normalization within each gene. First, we mean-normalize the read counts within each age group and serum treatment group (A, B, C, D). This is to account for baseline differences between sera collected from the different subjects. Second, we collapse replicates at each timepoint by calculating their means. Third, we calculate Z-Scores across all timepoints, within each age group. Note, these normalization procedures are to aid with visualization of the data and were not used as part of the statistical analyses.

Data and materials availability:

Sequencing data are deposited in Gene Expression Omnibus (NCBI) under accession number TBD. All additional data files are available upon request.

Acknowledgments:

We wish to extend our sincere gratitude to the study volunteers. Ms. LaVenia Banas provided excellent logistical study support. We thank Dr. Andrew Liu for the BMAL1-luc plasmid. We thank the RIA Biomarker Core of the Penn Diabetes Research Center, P30-DK19525 for

cortisol measurements. We thank Sara Bernardez-Noya and Rebecca Moore for input on analysis and data presentation. The project described was supported by the National Center for Research Resources and the National Center for Advancing Translational Sciences, National Institutes of Health, through Grant 5UL1TR001878 (A.S.) and National Heart, Blood, and Lung Institutes of Health, through Grant R00HL1472 (S.L.Z.). C.S. is the Robert L. McNeil Jr. Fellow in Translational Medicine and Therapeutics. A.S. is an investigator of the Howard Hughes Medical Institute. J.E.S. was supported by a training grant in Neuroscience (NIH T32-NS105607), an National Institutes of Health Diversity Supplement (NIH NS48471), and by a grant to the University of Pennsylvania from the Howard Hughes Medical Institute through the James H. Gilliam Fellowship for Advanced Study program. The funders had no role in study design, data collection and analysis, decision to publish, or preparation of the manuscript.

References

1. Monk, T. H., Buysse, D. J., Reynolds, C. F. & Kupfer, D. J. Inducing jet lag in older people: Adjusting to a 6-hour phase advance in routine. *Experimental Gerontology* **28**, 119–133 (1993).
2. Monk, T. H., Buysse, D. J., Carrier, J. & Kupfer, D. J. Inducing jet-lag in older people: Directional asymmetry. *Journal of Sleep Research* **9**, 101–116 (2000).
3. Hood, S. & Amir, S. The aging clock: circadian rhythms and later life. *Journal of Clinical Investigation* **127**, 437–446 (2017).
4. Farajnia, S. *et al.* Evidence for Neuronal Desynchrony in the Aged Suprachiasmatic Nucleus Clock. *J. Neurosci.* **32**, 5891–5899 (2012).
5. Nakamura, T. J. *et al.* Age-Related Decline in Circadian Output. *J Neurosci* **31**, 10201–10205 (2011).
6. Yamazaki, S. *et al.* Effects of aging on central and peripheral mammalian clocks. *Proc Natl Acad Sci U S A* **99**, 10801–10806 (2002).

7. Gerber, A. *et al.* Blood-Borne Circadian Signal Stimulates Daily Oscillations in Actin Dynamics and SRF Activity. *Cell* **152**, 492–503 (2013).
8. Katsimpardi, L. *et al.* Vascular and Neurogenic Rejuvenation of the Aging Mouse Brain by Young Systemic Factors. *Science* **344**, 630–634 (2014).
9. Ramanathan, C., Khan, S. K., Kathale, N. D., Xu, H. & Liu, A. C. Monitoring Cell-autonomous Circadian Clock Rhythms of Gene Expression Using Luciferase Bioluminescence Reporters. *JoVE (Journal of Visualized Experiments)* e4234 (2012) doi:10.3791/4234.
10. Pagani, L. *et al.* Serum factors in older individuals change cellular clock properties. *Proceedings of the National Academy of Sciences of the United States of America* (2011) doi:10.1073/pnas.1008882108.
11. Balsalobre, A., Damiola, F. & Schibler, U. A Serum Shock Induces Circadian Gene Expression in Mammalian Tissue Culture Cells. *Cell* **93**, 929–937 (1998).
12. Parsons, R., Parsons, R., Garner, N., Oster, H. & Rawashdeh, O. CircaCompare: a method to estimate and statistically support differences in mesor, amplitude and phase, between circadian rhythms. *Bioinformatics* **36**, 1208–1212 (2020).
13. Szklarczyk, D. *et al.* STRING v11: protein-protein association networks with increased coverage, supporting functional discovery in genome-wide experimental datasets. *Nucleic Acids Res* **47**, D607–D613 (2019).
14. Krämer, A., Green, J., Pollard, J. & Tugendreich, S. Causal analysis approaches in Ingenuity Pathway Analysis. *Bioinformatics* **30**, 523–530 (2014).
15. Holubiec, M. I., Gellert, M. & Hanschmann, E. M. Redox signaling and metabolism in Alzheimer's disease. *Front Aging Neurosci* **14**, 1003721 (2022).
16. Sehar, U., Rawat, P., Reddy, A. P., Kopel, J. & Reddy, P. H. Amyloid Beta in Aging and Alzheimer's Disease. *Int J Mol Sci* **23**, 12924 (2022).

17. Raulin, A.-C. *et al.* ApoE in Alzheimer's disease: pathophysiology and therapeutic strategies. *Mol Neurodegener* **17**, 72 (2022).
18. Chen, C.-Y. *et al.* Effects of aging on circadian patterns of gene expression in the human prefrontal cortex. *Proc Natl Acad Sci U S A* **113**, 206–211 (2016).
19. Kuintzle, R. C. *et al.* Circadian deep sequencing reveals stress-response genes that adopt robust rhythmic expression during aging. *Nat Commun* **8**, 14529 (2017).
20. Sato, S. *et al.* Circadian Reprogramming in the Liver Identifies Metabolic Pathways of Aging. *Cell* **170**, 664-677.e11 (2017).
21. Solanas, G. *et al.* Aged Stem Cells Reprogram Their Daily Rhythmic Functions to Adapt to Stress. *Cell* **170**, 678-692.e20 (2017).
22. Blacher, E. *et al.* Aging disrupts circadian gene regulation and function in macrophages. *Nat Immunol* **23**, 229–236 (2022).
23. Wolff, C. A. *et al.* Defining the age-dependent and tissue-specific circadian transcriptome in male mice. *Cell Reports* **42**, 111982 (2023).
24. Lesnefsky, E. J. & Hoppel, C. L. Oxidative phosphorylation and aging. *Ageing Research Reviews* **5**, 402–433 (2006).
25. Greco, M. *et al.* Marked aging-related decline in efficiency of oxidative phosphorylation in human skin fibroblasts. *The FASEB Journal* **17**, 1706–1708 (2003).
26. Duffield, G. E. *et al.* Circadian programs of transcriptional activation, signaling, and protein turnover revealed by microarray analysis of mammalian cells. *Curr Biol* **12**, 551–557 (2002).
27. Grundschober, C. *et al.* Circadian regulation of diverse gene products revealed by mRNA expression profiling of synchronized fibroblasts. *J Biol Chem* **276**, 46751–46758 (2001).
28. Hughes, M. E. *et al.* Harmonics of Circadian Gene Transcription in Mammals. *PLOS Genetics* **5**, e1000442 (2009).

29. Jang, C., Lahens, N. F., Hogenesch, J. B. & Sehgal, A. Ribosome profiling reveals an important role for translational control in circadian gene expression. *Genome Res* **25**, 1836–1847 (2015).
30. Patel, V. R., Eckel-Mahan, K., Sassone-Corsi, P. & Baldi, P. CircadiOmics: integrating circadian genomics, transcriptomics, proteomics and metabolomics. *Nat Methods* **9**, 772–773 (2012).
31. Zhang, R., Lahens, N. F., Ballance, H. I., Hughes, M. E. & Hogenesch, J. B. A circadian gene expression atlas in mammals: Implications for biology and medicine. *Proc Natl Acad Sci U S A* **111**, 16219–16224 (2014).
32. Pagani, L. *et al.* Serum factors in older individuals change cellular clock properties. *Proceedings of the National Academy of Sciences* **108**, 7218–7223 (2011).
33. Cornelissen, G. Cosinor-based rhythmometry. *Theor Biol Med Model* **11**, 16 (2014).
34. Refinetti, R., Lissen, G. C. & Halberg, F. Procedures for numerical analysis of circadian rhythms. *Biol Rhythm Res* **38**, 275–325 (2007).
35. Lahens, N. F. *et al.* Time-specific associations of wearable sensor-based cardiovascular and behavioral readouts with disease phenotypes in the outpatient setting of the Chronic Renal Insufficiency Cohort. *Digit Health* **8**, 20552076221107904 (2022).
36. Zhang, S. L. *et al.* A circadian clock regulates efflux by the blood-brain barrier in mice and human cells. *Nat Commun* **12**, 617 (2021).
37. Zielinski, T., Moore, A. M., Troup, E., Halliday, K. J. & Millar, A. J. Strengths and Limitations of Period Estimation Methods for Circadian Data. *PLOS ONE* **9**, e96462 (2014).
38. Dobin, A. *et al.* STAR: ultrafast universal RNA-seq aligner. *Bioinformatics* **29**, 15–21 (2013).
39. Yates, A. D. *et al.* Ensembl 2020. *Nucleic Acids Research* **48**, D682–D688 (2020).
40. Weger, B. D. *et al.* Systematic analysis of differential rhythmic liver gene expression mediated by the circadian clock and feeding rhythms. *Proceedings of the National Academy of Sciences* **118**, e2015803118 (2021).

41. Brooks, T. G. *et al.* Nitecap: An Exploratory Circadian Analysis Web Application. *J Biol Rhythms* **37**, 43–52 (2022).

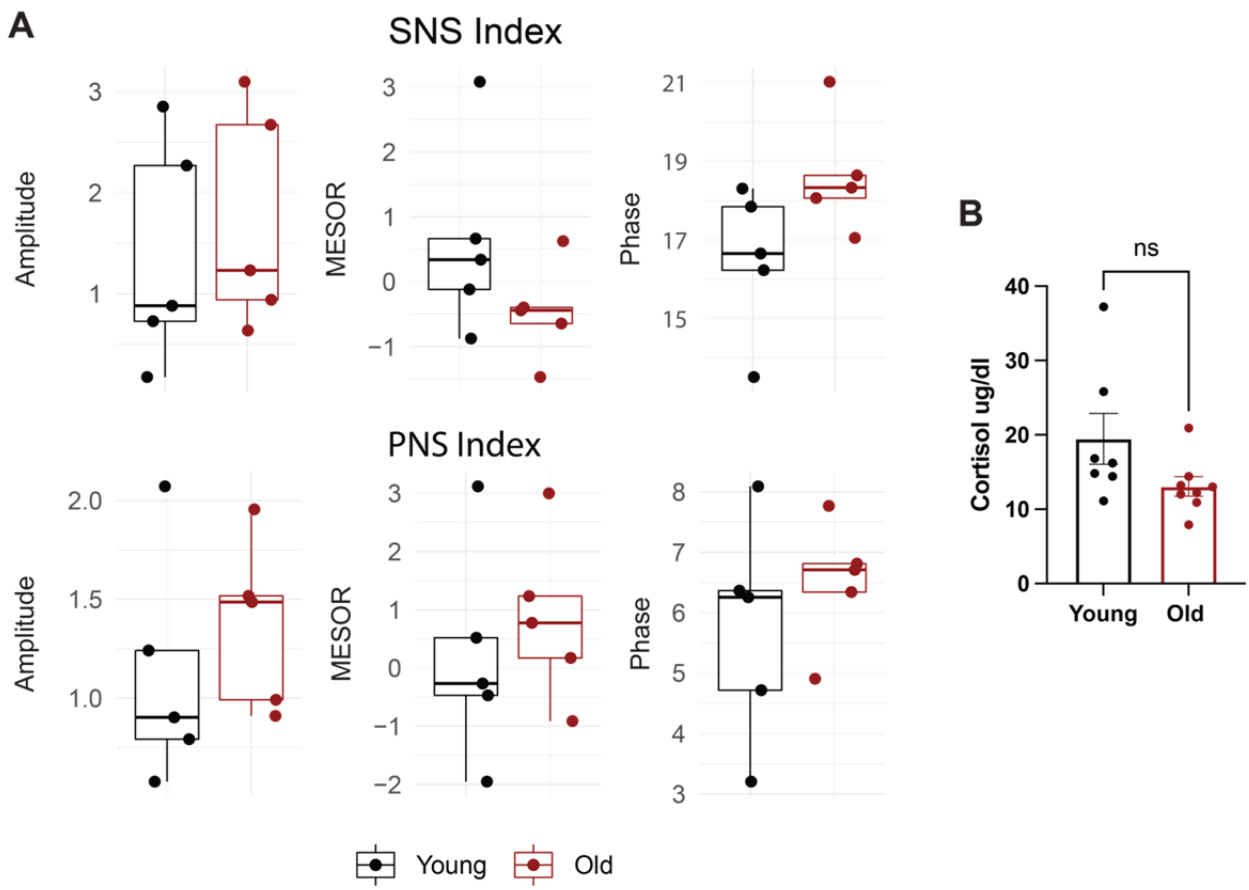

Fig S1. There are no significant differences in grip strength, sympathetic, parapsympathetic nervous system indices, or cortisol levels between young and old individuals

Sympathetic nervous system (SNS, A, top) and parasympathetic nervous system (PNS, A, bottom) indices were measured using EKG. Amplitude, MESOR, and Phase were calculated from the resulting oscillations and the Median, quartiles, and SEMs are shown. Dots represent individuals. P>0.05. N=5 per group. MESOR and amplitude were tested using Wilcoxon rank sum exact test, while phase was tested by Kuiper's two-sample test. Boxplot midlines correspond to median values, while the lower and upper hinges correspond to the first and third quartiles, respectively. Boxplot whiskers extend to the smallest/largest points within 1.5 * IQR (inter Quartile Range) of the lower/upper hinge **(A)**. Serum cortisol levels are not statistically different by unpaired t-test **(B**, N=7 young, 8 old **)**.

Table S1. Demographic information for subjects in the study.

Age Group	Sex	Age (y)	BMI (kg/m^2)	Total Sleep Time (TST) [h]
20-35	Male	30	25.9	6.4
	Female	30	28.7	7.4
	Female	25	23.7	6.6
	Male	28	25.0	9.7
	Female	28	21.2	6.9
	Male	28	25.2	7.4
	Male	28	25.9	9.3
Young	***Mean***	***28.1***	***25.1***	***7.7***
	SD	***1.7***	***2.3***	***1.3***
70-85	Male	76	22.3	5.8
	Male	75	28.8	7.8
	Female	73	32.4	7.7
	Female	74	26.4	7.5
	Male	73	21.5	6.6
	Male	71	26.7	11.3
	Male	74	27.2	7.0
	Male	70	26.8	6.7
Old	***Mean***	***73.3***	***26.5***	***7.6***
	SD	***2.0***	***3.4***	***1.7***

Total sleep time (TST) was calculated from ActiLife 6 determined in-bed and out-of-bed times averaged across nights with available actigraphy data (≥7 nights). Old (N=8), Y-young (N=7).

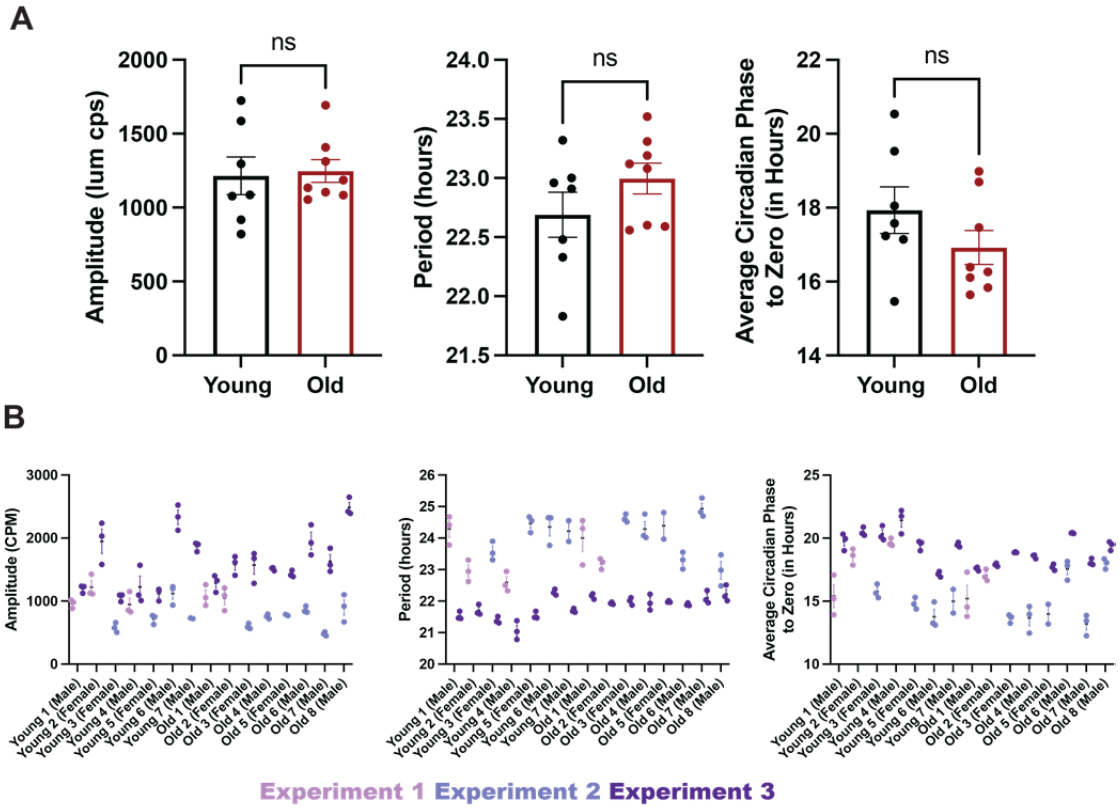

Fig S2: Young and old serum contain equivalent levels of cortisol and are equally effective at entraining cells in culture

(A) Cells synchronized with human serum from either young (N=7 subjects) or old (N=8 subjects) individuals did not show differences in amplitude (as measured in luminescence counts per second, bottom, left), period (bottom, middle), or phase (bottom, right). Data points represent average values for a specific patient's serum over 2 experiments with 2-3 replicates per experiment. A visual representation of the individual replicates averaged in A **(B)** Summary statistics are displayed as mean +/- SEM. Means compared by unpaired t-test. Despite individual and run to run variability, cells synchronized with human serum from either young (N=7 subjects) or old (N=8 subjects) individuals showed similar amplitude (top, left), period (top, right), and phase (bottom) of BMAL1-luciferase rhythms. Data points represent individual replicates within an experiment. Wells run in the same experiment are displayed in the same color. Each subject's sample was run in 2-3 replicates.

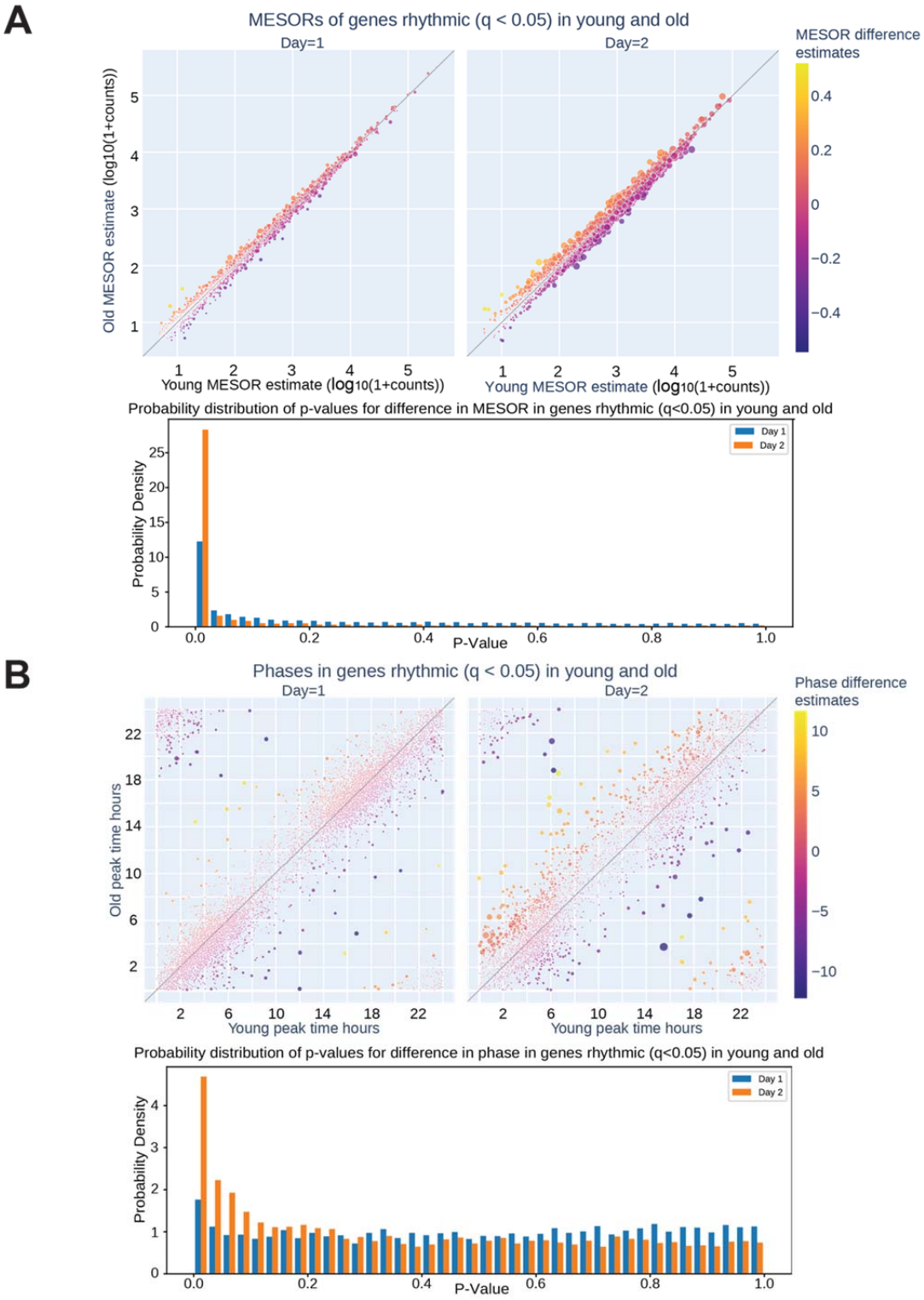

Fig S3. The circadian transcriptomes of cells synchronized with young or old sera deviate significantly on day two.

554 On day two of serum entrainment, young and old transcriptional rhythms differentiated.
555 CircaCompare analysis of RNA sequencing revealed that on Day 2 of serum entrainment
556 analysis (CT 36-58) the MESOR differences of cycling genes are larger between the cells
557 entrained with young or old serum **(A**, top**)**. Additionally, more genes were phase shifted in the
558 old serum condition compared to young serum on Day 2 **(B**, top**)**. The distribution of p-values
559 shows an enrichment of low p-values on Day 2 for both MESOR and phase differences (A,
560 bottom, B, bottom). The size of each circle in the scatter plots is proportional to $-\log_{10}q$, so the
561 bigger the circle, the smaller the q-value for the difference between young and old for each
562 metric.
563

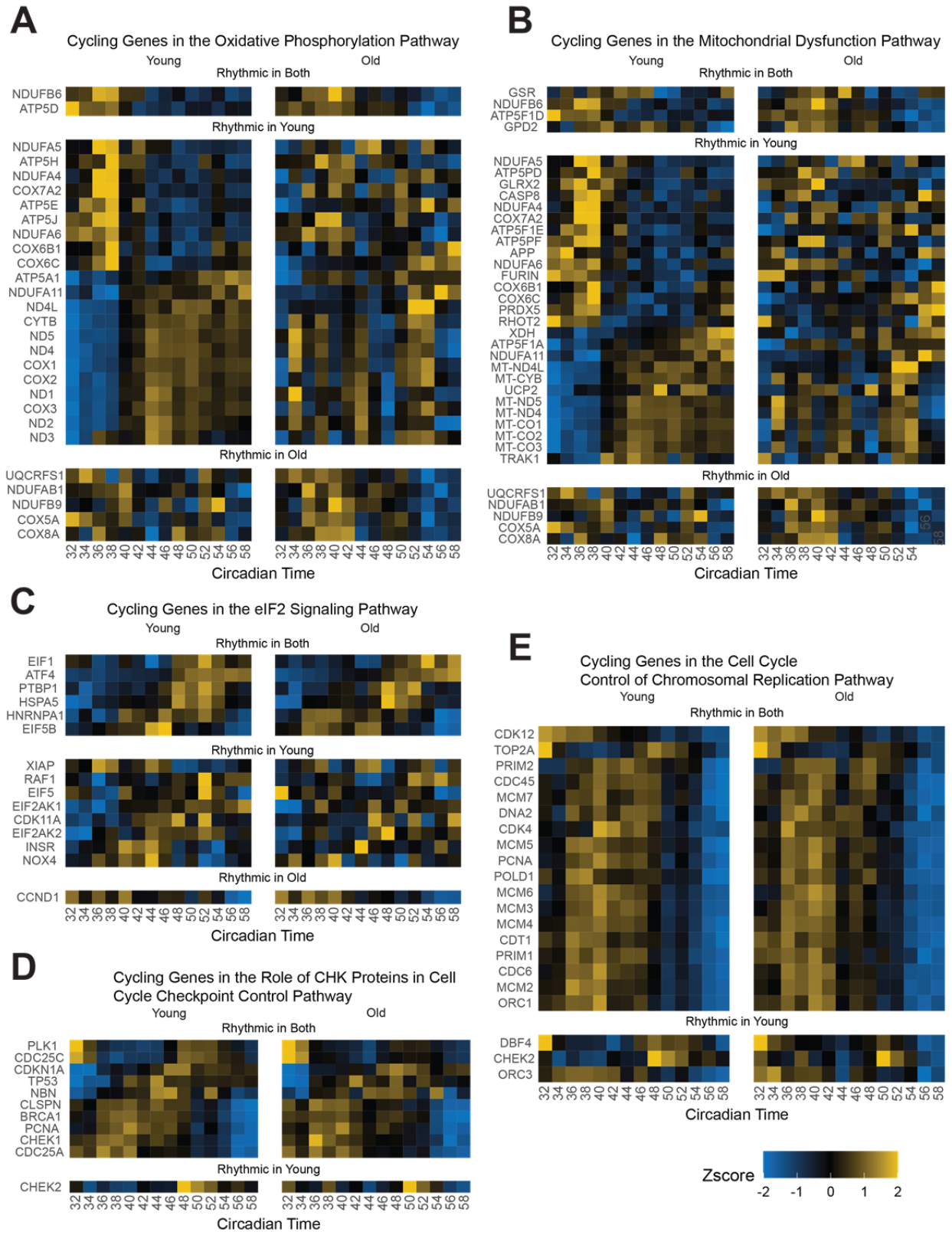
A
Cycling Genes in the Oxidative Phosphorylation Pathway
Young
Old
Rhythmic in Both
NDUFB6
ATP5D
Rhythmic in Young
NDUFA5
ATP5H
NDUFA4
COX7A2
ATP5E
ATP5J
NDUFA6
COX6B1
COX6C
ATP5A1
NDUFA11
ND4L
CYTB
ND5
ND4
COX1
COX2
ND1
COX3
ND2
ND3
Rhythmic in Old
UQCRFS1
NDUFAB1
NDUFB9
COX5A
COX8A
32 34 36 38 40 42 44 46 48 50 52 54 56 58
Circadian Time
B
Cycling Genes in the Mitochondrial Dysfunction Pathway
Young
Old
Rhythmic in Both
GSR
NDUFB6
ATP5F1D
GPD2
Rhythmic in Young
NDUFA5
ATP5PD
GLRX2
CASP8
NDUFA4
COX7A2
ATP5F1E
ATP5PF
APP
NDUFA6
FURIN
COX6B1
COX6C
PRDX5
RHOT2
XDH
ATP5F1A
NDUFA11
MT-ND4L
MT-CYB
UCP2
MT-ND5
MT-ND4
MT-CO1
MT-CO2
MT-CO3
TRAK1
Rhythmic in Old
UQCRFS1
NDUFAB1
NDUFB9
COX5A
COX8A
32 34 36 38 40 42 44 46 48 50 52 54 56 58
Circadian Time
C
Cycling Genes in the eIF2 Signaling Pathway
Young
Old
Rhythmic in Both
EIF1
ATF4
PTBP1
HSPA5
HNRNPA1
EIF5B
Rhythmic in Young
XIAP
RAF1
EIF5
EIF2AK1
CDK11A
EIF2AK2
INSR
NOX4
Rhythmic in Old
CCND1
32 34 36 38 40 42 44 46 48 50 52 54 56 58
Circadian Time
D
Cycling Genes in the Role of CHK Proteins in Cell Cycle Checkpoint Control Pathway
Young
Old
Rhythmic in Both
PLK1
CDC25C
CDKN1A
TP53
NBN
CLSPN
BRCA1
PCNA
CHEK1
CDC25A
Rhythmic in Young
CHEK2
32 34 36 38 40 42 44 46 48 50 52 54 56 58
Circadian Time
E
Cycling Genes in the Cell Cycle Control of Chromosomal Replication Pathway
Young
Old
Rhythmic in Both
CDK12
TOP2A
PRIM2
CDC45
MCM7
DNA2
CDK4
MCM5
PCNA
POLD1
MCM6
MCM3
MCM4
CDT1
PRIM1
CDC6
MCM2
ORC1
Rhythmic in Young
DBF4
CHEK2
ORC3
32 34 36 38 40 42 44 46 48 50 52 54 56 58
Circadian Time
Zscore
-2 -1 0 1 2

564

565

566 **Fig S4: Oxidative phosphorylation genes and chromosomal replication genes are**

567 **affected by entrainment with old serum**

568 Additional pathway analysis employing IPA further emphasizes finding with STRING analysis.

569 Genes identified by IPA analysis to be associated with oxidative phosphorylation/mitochondrial

570 dysfunction and eIF2 genes lose rhythmicity with age (BIC >0.75) **(A, B, C)**. Cell cycle

571 checkpoint control (CHK proteins) **(D)** and chromosomal replication genes **(E)** maintain their

572 cycling in the aged condition, which is consistent with the continued division of cells.

573

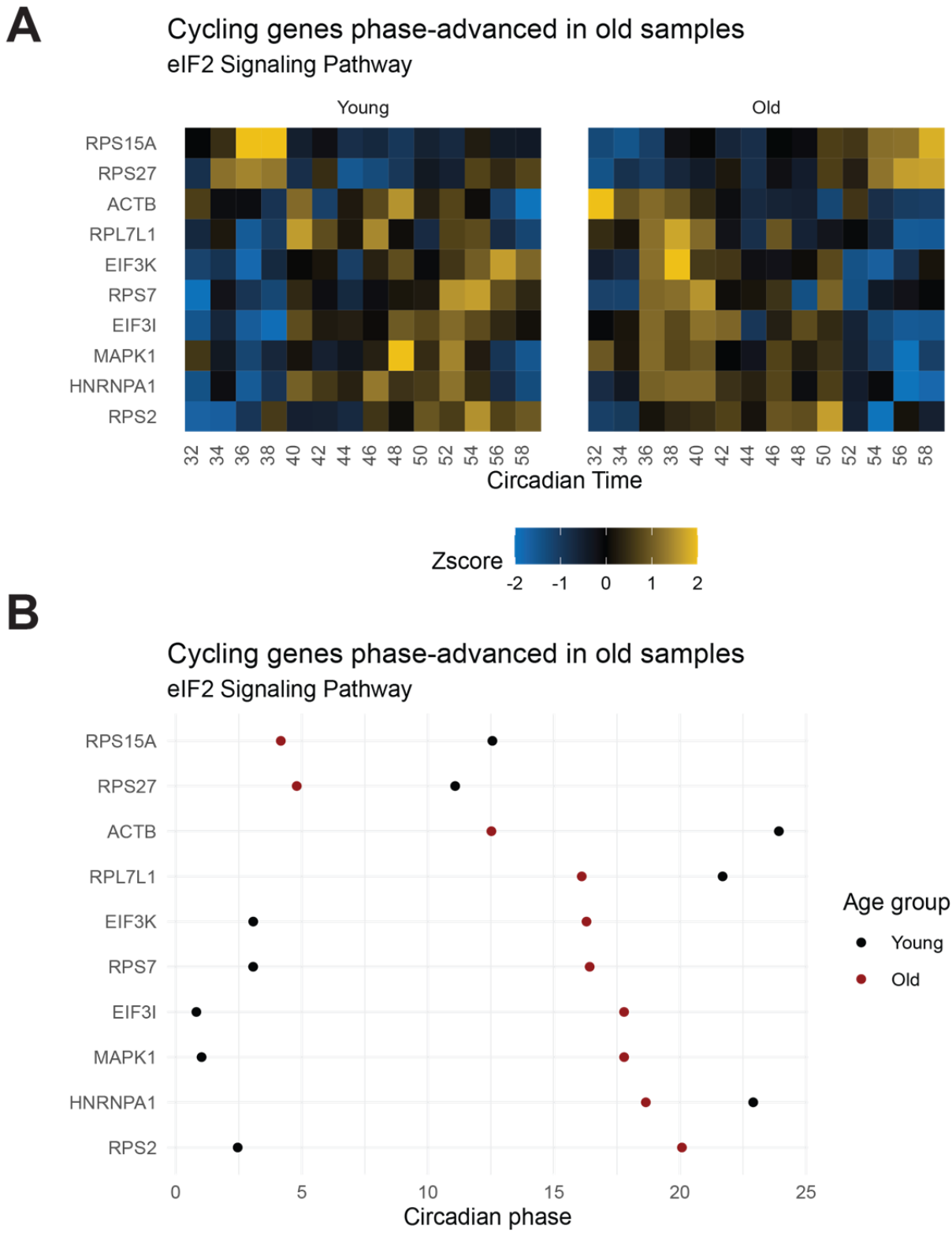
A
Cycling genes phase-advanced in old samples
eIF2 Signaling Pathway
Young
Old
RPS15A
RPS27
ACTB
RPL7L1
EIF3K
RPS7
EIF3I
MAPK1
HNRNPA1
RPS2
32 34 36 38 40 42 44 46 48 50 52 54 56 58
Circadian Time
Zscore
-2 -1 0 1 2
B
Cycling genes phase-advanced in old samples
eIF2 Signaling Pathway
RPS15A
RPS27
ACTB
RPL7L1
EIF3K
RPS7
EIF3I
MAPK1
HNRNPA1
RPS2
0 5 10 15 20 25
Circadian phase
Age group
Young
Old

578 **Fig S5: eIF2 signaling pathway genes that maintain cycling with age phase advance in**
579 **the old serum condition**
580
581 From the IPA analyses, the eIF2 signaling pathway was enriched (BIC >0.75) in two datasets:
582 1) genes cycling in the young sera and not the old and 2) cycling genes phase-advanced in the
583 old sera (q<0.05). A significant number of genes that maintain rhythmicity in the old sera
584 condition are phase advanced as visualized in the heat map **(A)** or plot of peak phase **(B)**. As
585 the eIF2 pathway is involved in protein translation, this suggests that the timing of protein
586 translation is phase advanced in the older serum and/or less rhythmic.
587

Gene	Symbol	Old_mesor_estimate	Young_mesor_estimate
ENSG00000014138	POLA2	1.942220257	2.030676546
ENSG00000062822	POLD1	2.727523056	2.828026817
ENSG00000073111	MCM2	3.003984606	3.115331295
ENSG00000076003	MCM6	3.124116273	3.203138512
ENSG00000085840	ORC1	2.177440998	2.305154417
ENSG00000091651	ORC6	2.415062674	2.513336383
ENSG00000093009	CDC45	2.428834807	2.540049538
ENSG00000094804	CDC6	2.566892644	2.679401971
ENSG00000097046	CDC7	2.279003902	2.377425914
ENSG00000100297	MCM5	3.17577594	3.288560637
ENSG00000101868	POLA1	2.640718445	2.728951631
ENSG00000104738	MCM4	3.310670684	3.413600036
ENSG00000112118	MCM3	3.168296215	3.269321473
ENSG00000117748	RPA2	2.754645539	2.798914718
ENSG00000131747	TOP2A	3.722304752	3.798890616
ENSG00000132383	RPA1	3.238584015	3.287556646
ENSG00000132646	PCNA	3.232760966	3.321439626
ENSG00000135446	CDK4	3.143303063	3.172936739
ENSG00000138346	DNA2	2.113453067	2.238476228
ENSG00000146143	PRIM2	2.620994795	2.675363852
ENSG00000164815	ORC5	2.361538047	2.414675015
ENSG00000166508	MCM7	3.381394362	3.482444492
ENSG00000167258	CDK12	3.10241713	3.129181459
ENSG00000167513	CDT1	2.474002764	2.590319547
ENSG00000198056	PRIM1	2.116803844	2.231962095

Table S2: Genes with decreased MESOR in the IPA cell cycle control of chromosomal replication pathway

Table of genes that are rhythmic in both conditions with a decreased MESOR with old serum treatment compared to young serum treatment by CircaCompare. All genes are involved in the cell cycle/DNA replication pathway.

598

Gene	Symbol	Old_mesor_estimate	Young_mesor_estimate
ENSG00000001630	CYP51A1	2.040377336	1.871207095
ENSG00000079459	FDFT1	3.330291993	3.19001773
ENSG00000104549	SQLE	3.116822033	2.950386727
ENSG00000110921	MVK	2.530172998	2.4121956
ENSG00000112972	HMGCS1	2.93111747	2.696086286
ENSG00000113161	HMGCR	3.011982868	2.833316048
ENSG00000116133	DHCR24	3.506294106	3.343492054
ENSG00000120437	ACAT2	2.71791125	2.58109012
ENSG00000132196	HSD17B7	1.940436315	1.782521965
ENSG00000147383	NSDHL	2.540302415	2.468852126
ENSG00000160285	LSS	3.486802994	3.411431601
ENSG00000160752	FDPS	3.143592562	3.081359846
ENSG00000167508	MVD	2.819963909	2.68386468
ENSG00000172893	DHCR7	2.990620862	2.797567922

599

600 **Table S3: Genes with increased MESOR in the IPA cholesterol biosynthesis pathway**

601 Table of genes that are rhythmic in both conditions with a decreased MESOR with old serum

602 treatment compared to young serum treatment by CircaCompare. All genes are involved in the

603 cholesterol biosynthesis pathway.

604

605

606